

Regiospecific Structure, Degradation, and Functionalization of Polyperoxides Prepared from Sorbic Acid Derivatives with Oxygen

Yuko Sugimoto, Shuji Taketani, Tomoaki Kitamura, Daisaku Uda, and Akikazu Matsumoto*

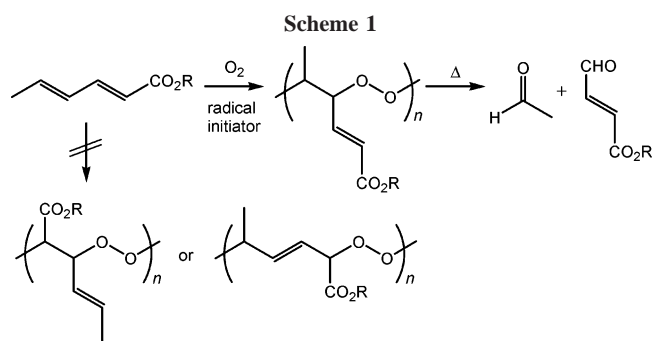
Department of Applied Chemistry, Graduate School of Engineering, Osaka City University, Sugimoto, Sumiyoshi-ku, Osaka 558-8585, Japan

Received August 10, 2006; Revised Manuscript Received September 25, 2006

ABSTRACT: We have fabricated degradable polyperoxides (**PP**) consisting of well-controlled 5,4-repeating units using various sorbic acid derivatives and molecular oxygen by an alternating radical copolymerization process. The **PP** obtained from the sorbic esters decompose via a radical chain reaction mechanism, leading to the formation of controlled low-molecular-weight products. In contrast, **PP** from some amide derivatives include an irregular chain structure, resulting in a more complicated degradation behavior. The theoretical calculations account for the selectivity in the two-step regiospecific propagation depending on the monomer structure. We have demonstrated the synthesis of functional **PP** based on two methods: one is the copolymerization of functional diene monomers with oxygen, and the other is the polymer reaction of **PP** including an azide group with a functional alcohol.

Introduction

Molecular oxygen, having a triplet electronic structure in the ground state, reacts with various kinds of unsaturated compounds, such as diene monomers, to provide polyperoxides (**PP**) consisting of both 1,2- and 1,4-repeating structures.^{1–11} The obtained **PP** includes a labile O–O bond in their main chain, differing from common vinyl and diene polymers. We have previously reported that **PP** can be conveniently produced by the radical copolymerization of alkyl sorbates (**1**) with oxygen under mild polymerization conditions, that is, ambient pressure and temperature in the presence of a radical initiator.¹² The obtained **PP** has a highly regular chain structure consisting of an exclusive 5,4-unit as the alternating repeating diene unit and produces acetaldehyde and a fumaraldehyde monoalkyl ester as the degradation products upon heating (Scheme 1). **PP** readily

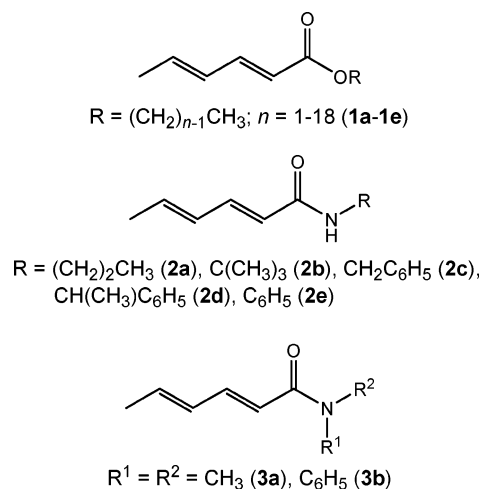


degrades via a radical chain mechanism using various stimuli such as UV irradiation, the addition of a base, and enzymatic reaction other than thermal degradation.¹³ Therefore, it is expected as the new kind of degradable polymer with significant potential in the fields of adhesion, coating, environment, and medicinal chemistry. We already reported some preliminary results regarding the syntheses of environmentally friendly **PP** that avoid the evolution of volatile and toxic degradation products,^{13,14} water-soluble **PP** which exhibit an LCST (lower

critical solution temperature)-type phase separation,¹⁵ degradable **PP** gels using bifunctional diene monomers,¹⁶ and poly(lactic acid) with a branched or network structure containing **PP** repeating units as the thermally degradable junctions.¹⁷

The highly controlled regiostructure of the **PP** chain is necessary for controlling the degradation and its reaction products. Recently, we succeeded in explaining the high regioselectivity during the propagation of methyl sorbate and its related derivatives using the density functional theory (DFT) calculations.¹⁴ In this paper, we report the synthesis and degradation of **PP** obtained from various ester and amide derivatives of sorbic acid, as are shown in Chart 1. The

Chart 1



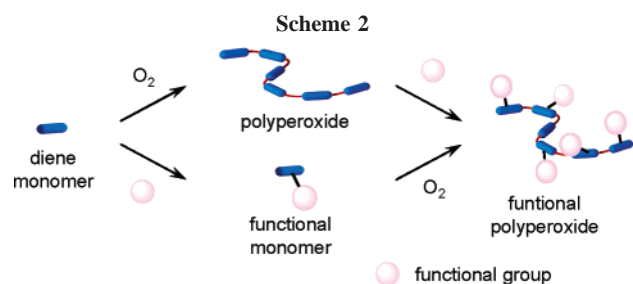
polymerization reactivity and the selectivity of the propagation reaction during the copolymerization are discussed on the basis of the results of the theoretical calculations as well as the repeating structure and degradation properties of the resulting **PP**. To use **PP** as functional polymers, we tried to introduce other functional groups into the **PP**. There are two methods for introducing a functional group (Scheme 2): one is the polymerization of a diene monomer with a functional group, and the other is the pathway via a polymer reaction. We now describe

* Corresponding author: Fax +81-6-6605-2981; e-mail matsumoto@ a-chem.eng.osaka-cu.ac.jp.

Table 1. Synthesis of PP from Sorbic Ester and Amide Derivatives (1–3) and Their Thermal Degradation Properties

	substituent	polymerization				TGA			DTA		
		yield (%)	$M_n \times 10^{-3}$	M_w/M_n	P_n	T_{95} (°C)	T_{50} (°C)	residue at 450 °C (%)	T_{init} (°C)	T_{max} (°C)	$-\Delta H$ (kJ/unit)
1a	methyl	43.5	3.2	1.6	20	119.5	148.2	4.9	107.9	147.5	187
1b	<i>n</i> -butyl	26.8	4.2	1.6	21	113.8	152.9	5.1	105.7	142.7	148
1c	decyl	28.6	7.4	1.6	26	141.4	172.7	6.8	104.5	148.1	179
1d	tetradecyl	21.2	7.5	1.4	22	145.4	211.2	5.2	106.3	146.2	163
1e	octadecyl	30.4	8.6	1.4	22	161.8	247.7	8.7	106.2	152.2	191
2a	<i>N</i> - <i>n</i> -propyl	70.3	0.9	1.3	5	136.1	258.8	17.1	88.4	137.6	145
2b	<i>N</i> - <i>tert</i> -butyl	55.9	1.6	1.4	8	127.9	191.9	11.8	87.0	140.7	189
2c	<i>N</i> -benzyl	51.2	1.9	1.4	8	140.2	328.7	24.1	100.8	140.2	189
2d	<i>N</i> -1-phenylethyl	54.5	1.7	1.5	7	148.5	302.1	21.7	106.8	140.2	182
2e	<i>N</i> -phenyl	55.1	2.3	1.5	10	144.2	338.6	29.0	108.4	140.2	212
3a	<i>N,N</i> -dimethyl	65.9	0.8	1.2	4	130.6	251.8	25.6	86.2	120.6	252
3b	<i>N,N</i> -diphenyl	25.6	2.5	1.5	8	137.8	254.4	14.9	101.5	136.7	212

the syntheses of functional PP by the copolymerization of several functional ester and amide monomers with oxygen and by the polymer reaction of PP including a reactive azide group with some functional alcohols.



Experimental Section

General Methods. The number-average molecular weight (M_n), polydispersity (M_w/M_n), and the number-average degree of polymerization (P_n) were determined by GPC at 30 °C in THF using a Tosoh GPC-8000 series system and calibrated with standard polystyrenes. The NMR spectra were recorded on a JEOL JNM A-400 spectrometer. The thermogravimetric and differential thermal analyses (TGA and DTA) were carried out using a SEIKO TG/DTA 6200 at the heating rate of 10 °C/min in a nitrogen stream. The sample weight was ~1 mg. All DFT calculations were carried out using a Spartan'04 software package.

Materials. The solvents were used after distillation. 2,2'-Azobis(4-methoxy-2,4-dimethylvaleronitrile) (AMVN) was purchased from Wako Pure Chemical Industries, Ltd., Japan, and used after recrystallization from methanol. Commercial methyl sorbate (Tokyo Kasei Kogyo Co., Ltd., Japan) was used after distillation under reduced pressure. The other monomers were prepared from sorbic acid or sorbic acid chloride and the corresponding alcohols and amines. The products were distilled under reduced pressure or recrystallized. Detailed procedures for the monomer synthesis and spectral data are shown in the Supporting Information.

Polymerization. The polymerization was carried out in a Pyrex tube with bubbling oxygen at 30 °C in the presence of AMVN (monomer/initiator = 50/1 by weight). 1,2-Dichloroethane was used as the solvent (monomer/solvent = 1/1–1/16 by weight). After the polymerization, the contents of the tube were poured into a large amount of precipitant to isolate the resulting polymer. A mixture of cyclohexane and *tert*-butyl methyl ether (1/1 by volume) for PP-2, diethyl ether and *n*-hexane (1/1 by volume) for PP-5a, and diethyl ether and *n*-hexane (1/3 by volume) for PP-5c were used. For the other cases, *n*-hexane was used as the precipitant. During all the isolation and purification procedures, the peroxide polymers should be treated without overheating and contact with any reducing agent and metal to avoid explosive decomposition, although they can be handled using conventional procedures at room temperature. Especially PP-5a should be carefully handled because of its high

reactivity and large exothermic heat during degradation. See also the procedure for the treatment of the low-molecular-weight organic peroxides in a textbook.

Results and Discussion

Synthesis of PP. The radical copolymerization of alkyl sorbates (1) as well as *N*-substituted and *N,N*-disubstituted sorbamides (2 and 3) with oxygen was carried out in 1,2-dichloroethane using AMVN as a radical initiator at atmospheric pressure and 30 °C; monomer/solvent = 1/1 for 1 and 1/8 for 2 and 3 by weight and monomer/AMVN = 50/1 by weight. The polymer was isolated with the appropriate precipitant and dried in vacuo at room temperature. M_n and M_w/M_n were determined by GPC calibrated with standard polystyrenes. NMR spectroscopy confirmed the alternating structure of the copolymers obtained from all the monomers. Table 1 summarizes the isolated polymer yield, M_n , M_w/M_n , and P_n of the resulting polymers, together with the thermal analysis results.

The M_n values for PP-1 increased with an increase in the carbon number of the alkyl groups from 3.2 to 8.6×10^3 , while P_n was constant. PP-1 was isolated as the tacky or powdery solids according to the size of the ester alkyl groups. As expected, the T_g value decreased from -10.7 °C for the methyl ester (PP-1a) to -53.5 °C for the decyl ester (PP-1c). For PP-1 with a longer alkyl side chain, crystallization of the side chains was observed; $T_c = 23.7$ °C, $T_m = 12.4$ °C, and $\Delta H_m = 20.0$ kJ/unit for PP-1d, and $T_c = 52.3$ °C, $T_m = 47.1$ °C, and $\Delta H_m = 32.2$ kJ/unit for PP-1e, where T_c , T_m , and ΔH_m are the crystallization and melting temperatures of the polymer side chains and the enthalpy change for melting, respectively. The side chains of PP-1e includes 10 methylene units as the crystallizable side chain as well as eight methylene units that cannot crystallize even at a low temperature per one repeating unit of the polymer. The crystallization behavior of the long alkyl side chain of PP is similar to those for other comblike polymers.¹⁸

PP-2 and PP-3 were isolated as powders, except for the tacky PP-3a. The polymer yield was 51–70%, being higher than the yield for PP-1 (21–44%). 3b exceptionally provided a low yield because of the significant steric hindrance of the *N*-phenyl group. A change in the resonance structure of 3b was confirmed by the shift of peaks in the ¹H NMR spectrum (Supporting Information). All the M_n values for PP-2 and PP-3 were lower than those for PP-1. This is due to the more frequently occurring chain transfer to the *N* substituents in addition to a low monomer concentration as the limited polymerization conditions. The concentration of the amide monomers was low (monomer/solvent = 1/8 by weight) due to the low solubility of the solid monomers compared to the polymerization conditions (monomer/solvent = 1/1) for 1.

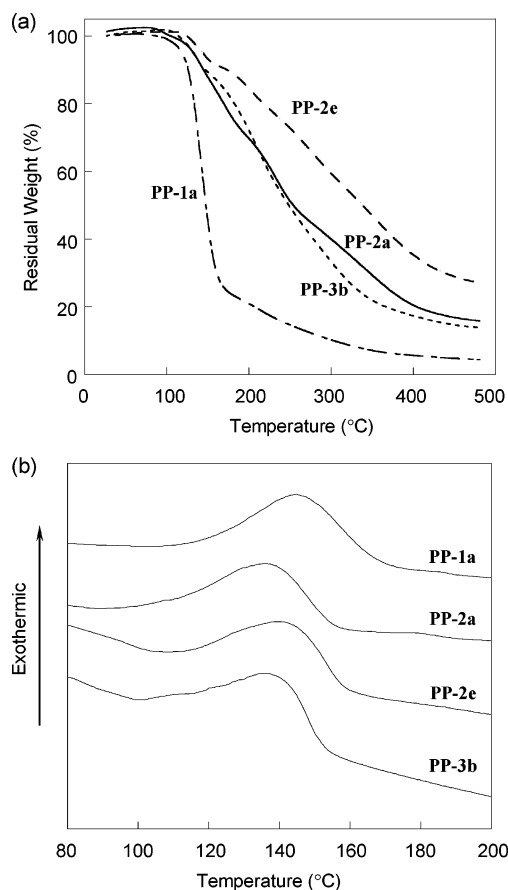


Figure 1. (a) TGA and (b) DTA curves for **PP-1a**, **PP-2a**, **PP-2e**, and **PP-3b** in a nitrogen stream at the heating rate of 10 °C/min.

Table 2. Copolymerization of **1a** with **2d** in the Presence of Oxygen

1a mol % in feed	yield (%)	$M_n \times 10^{-3}$	M_w/M_n	1a mol % in polymer
10.0	43.1	1.7	1.3	4.0
30.0	47.6	2.0	1.4	13.0
50.0	31.3	1.9	1.4	28.3
70.0	26.8	1.9	1.5	53.4
90.0	26.2	1.9	1.4	82.3

To directly examine the polymerization reactivity of the amide and ester derivatives, the copolymerization of **2d** with **1a** was carried out in the presence of oxygen. Both monomers exclusively underwent cross-propagation with oxygen; in other words, each homo-propagation of **2d** and **1a** and cross-propagation between **2d** and **1a** are negligible in this ternary copolymerization system consisting of **2d**, **1a**, and oxygen. As summarized in Table 2, the content of **1a** in the copolymer was always lower than that in the feed, indicating the higher monomer reactivity of **2d** than **1a**. From the comonomer–copolymer composition relationship, we determined the monomer reactivity ratios as follows: $r_1(\mathbf{2d}) = 1.12 \pm 0.1$ and $r_2(\mathbf{1a}) = 0.79 \pm 0.07$, using the integral form of the Mayo–Lewis equation.¹⁹ No penultimate group effect was observed in this case; that is, the product of r_1 and r_2 is equal to unity within the experimental error ($r_1 r_2 = 0.88 \pm 0.14$). The Q and e values were calculated as follows: by combination with the reported monomer reactivity ratios²⁰ $Q_2(\mathbf{1a}) = 0.79$ and $e_2(\mathbf{1a}) = 0.44$, $Q_1(\mathbf{2d}) = 1.17$ and $e_1(\mathbf{2d}) = 0.79$. These Q and e values suggest that a sorbamide monomer is a more conjugating and electron-accepting monomer than sorbate, leading to the faster addition of an electrophilic peroxy radical and the consequent high polymer yield.

Thermal Degradation of PP. The degradation temperature was determined from the results of the TGA/DTA measurements

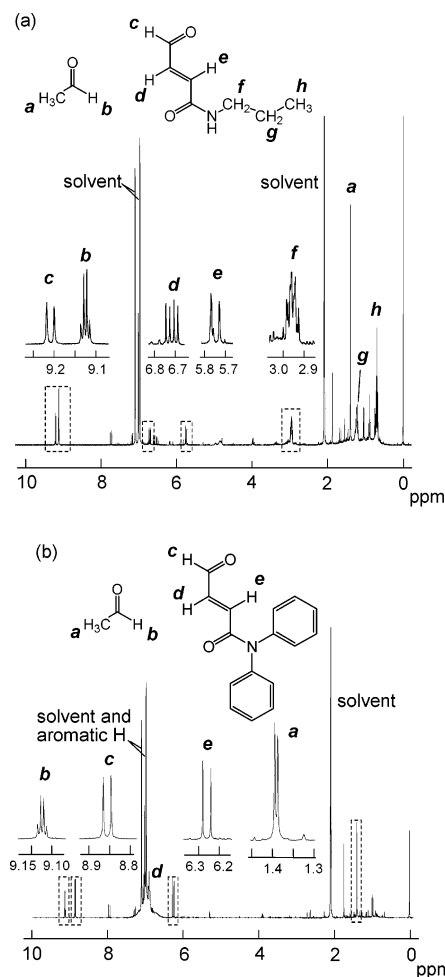


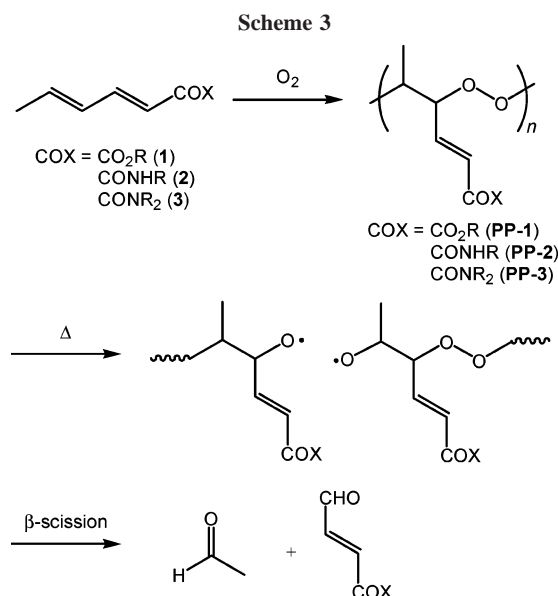
Figure 2. ¹H NMR spectra of the degradation products obtained from (a) **PP-2a** and (b) **PP-3b**. Degradation conditions: 100 °C, 1 h, toluene-*d*₈. The measurements were carried out at the ambient temperature after degradation.

in a nitrogen stream at the heating rate of 10 °C/min. The typical TGA and DTA curves are shown in Figure 1. These results are summarized in Table 1, where T_{95} and T_{50} are the 95 and 50 wt % temperatures, respectively, determined by TGA. The initial and maximum degradation temperatures, T_{init} and T_{max} , respectively, were estimated from the onset and peak temperatures of an exothermic peak in the DTA curve. The weight-loss temperature (T_{95} and T_{50} in TGA) apparently increased when the carbon number in the ester alkyl groups of **PP-1** increased. In the DTA experiments, however, the T_{init} and T_{max} values agreed well with each other for all the **PP-1**; $T_{\text{init}} = 104\text{--}108$ °C and $T_{\text{max}} = 142\text{--}152$ °C. Negative and high values for the heat of degradation (ΔH) indicate the totally exothermic degradation process including the cleavage of the peroxide linkages in the polymer chain, followed by the successive β -scission as the chain reactions. As is shown in the TGA curves, the degradation behaviors of **PP-2** and **PP-3** were more complicated than that of **PP-1**. Therefore, we further examined the isothermal degradation products by NMR spectroscopy. The degradation of **PP** was carried out in toluene-*d*₈ in a sealed tube at 100 °C for 1 h. The ¹H NMR spectra in Figure 2 include acetaldehyde and the corresponding fumaraldehyde monoamide derivatives as the major products from the thermal degradation of **PP-2** and **PP-3**, similar to those for **PP-1**^{12,13} (Scheme 3). In some cases, however, other products were also observed upon heating. For example, the *N*-propyl and *N,N*-dimethyl derivatives (**PP-2a** and **PP-3a**, respectively) produced other products

Table 3. DFT Calculation for Electron Density, Enthalpy Change (ΔH_A and ΔH_B) for Addition of Methyl Peroxy Radical to Diene, and BDE of C–O Bond of Peroxy Radicals^a

monomer	X	Mulliken atomic charge				ΔH_A (kcal/mol)	ΔH_B (kcal/mol)	$\Delta H_B - \Delta H_A$ (kcal/mol)	BDE _{5,4} (kcal/mol)	BDE _{5,2} (kcal/mol)
		C5	C4	C3	C2					
1a	CO ₂ CH ₃	−0.155	−0.178	−0.130	−0.327	−9.95	−0.87	9.08	15.17	9.45
2a	CONH(CH ₂ CH ₂ CH ₃)	−0.158	−0.179	−0.139	−0.351	−9.95	−6.62	3.33	14.25	12.91
3a	CON(CH ₃) ₂	−0.157	−0.181	−0.125	−0.364	−10.24	−3.56	6.68	15.73	12.01
3b	CON(C ₆ H ₅) ₂	−0.157	−0.181	−0.129	−0.362	−9.82	−0.71	9.11	15.67	10.08

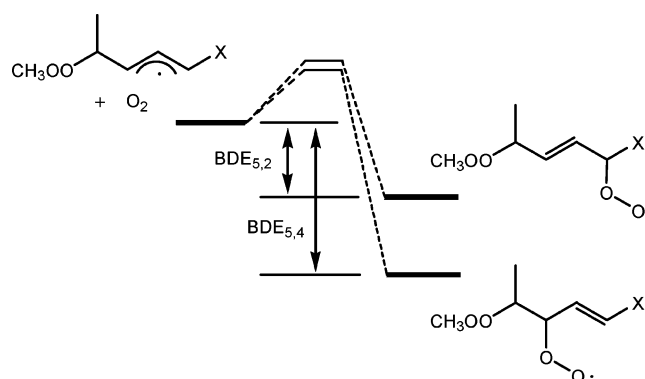
^a Calculation of enthalpy change was carried out at the (RO)B3LYP/6-311**/(U)B3LYP/6-311* level of theory. ΔH_A and ΔH_B are the enthalpy change for the reactions via paths A and B, respectively, in Scheme 4. For BDE_{5,4} and BDE_{5,2}, see Figure 3.



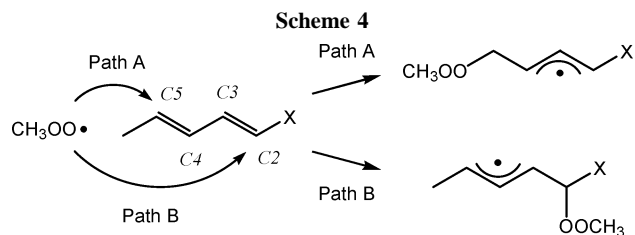
besides the expected two aldehydes. The residue of the **PP-2** and **PP-3** (12–29%) after degradation was higher than those for the **PP-1** (5–9%). The **PP-2b** and **PP-3b**, which have the *N*-tert-butyl and *N,N*-diphenyl substituents, respectively, were converted to the expected aldehydes as the main products, and the residual weight was low (11.8–14.9%). These results indicate the frequent occurrence of hydrogen abstraction from the *N*-methyl or methylene groups during the degradation, leading to the complicated degradation mechanism.

Propagation Mechanism. During the radical copolymerization of **1–3** with oxygen, a highly regiospecific propagation occurs except for some amide derivatives. For controlling the reaction and the structure of the products during degradation, the well-controlled repeating structures of **PP**, including the highly alternating and 5,4-repeating units, are required. In general, however, regiospecific propagation of diene monomers is difficult during the free-radical polymerization in solution. The selectivity observed during the copolymerization of the sorbic derivatives with oxygen cannot be simply interpreted by the electron affinity of a peroxy radical to a diene monomer and by the nature of a propagating allyl radical as the carbon-centered radical. We carried out theoretical calculations using a DFT method at the B3LYP level with the basis set of 6-311G* in order to clarify the selectivity of the propagation reactions. The results are shown in Table 3.

On the basis of the calculation results for the Mulliken atomic charges, the electron density on the C2 carbon was much higher than that on C5 for all the monomers. Actually, the exclusive addition of a peroxy radical on the C5 carbon was observed. Therefore, we examined the stability of the resulting allyl radicals by the addition of a peroxy radical to a diene monomer to explain the experimental results. We calculated the difference in the heat of formation (ΔH) during the reactions of a methyl

**Figure 3.** Energy diagram for the reaction of allyl radicals produced from diene monomers with molecular oxygen, resulting in the formation of 5,2- and 5,4-adduct radicals and their reverse reactions.

peroxy radical to diene monomers via two possible pathways. Paths A and B are the addition of the radical to the C5 and C2 carbons of a diene monomer, respectively. The calculations provided the result that all the reactions are exothermic (ΔH are negative) and the absolute values for path A were greater than those for path B. The values of $\Delta H_B - \Delta H_A$ were 3.33–9.11 kcal/mol, indicating the preference of the more stabilized structure of the allyl radicals formed via path A by conjugation to a carbonyl group. On the basis of the calculation results for **2a** and **3a**, we confirmed the possibility of the both addition reactions due to a smaller difference in the ΔH values for the two pathways.



The selectivity for the reaction of a delocalized allyl radical with molecular oxygen is discussed on the basis of bond dissociation energies (BDE) of the adducts. The 5,4- and 5,2-propagations provide the peroxy radicals containing different BDE values for the carbon-to-oxygen bond. The reaction of the carbon-centered radical with oxygen is reversible, and the BDE value is closely related to the rate constant of the β -dissociation (k_β).²¹ The greater the BDE values of C–O, the smaller the k_β values. We calculated the enthalpies of the formation of the 5,2- and 5,4-adducts, as shown in the schematic energy diagram in Figure 3. These results are summarized in Table 3.

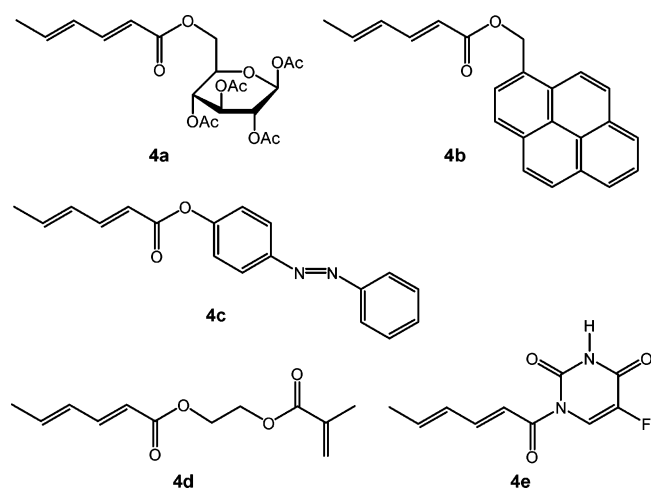
The BDE_{5,4} values were independent of the structure of X, while the BDE_{5,2} values for the **2a** and **3a** (12.0–12.9 cal/mol) were larger than that of **1a** (9.5 cal/mol): in the order of 9.45 kcal/mol for **1a**, 10.08 kcal/mol for **3b**, 12.01 kcal/mol for **3a**, and 12.91 kcal/mol for **2a**. The dissociation of the peroxy radical

Table 4. Copolymerization of Functional Sorbic Derivatives (4 and 5) with Oxygen^a

monomer	monomer/solvent ratio by weight	yield (%)	$M_n \times 10^{-3}$	M_w/M_n	P_n	repeating unit of diene
4a	1/4	20.1	2.6	1.2	6	5,4-
4b	1/16	16.9	1.8	1.3	5	5,4-
4c	1/8	24.0	1.9	1.4	6	5,4-
4d	1/1	39.6	<i>b</i>	<i>b</i>	<i>b</i>	
4e	1/4	19.8	1.0	1.2	4	predominantly 5,4-
5a	1/1	25.3	2.8	2.1	16	
5b	1/1	<i>b</i>	<i>b</i>	<i>b</i>	<i>b</i>	
5c	1/6	41.3	3.6	1.5	18	5,4-, 5,2-, and 2,3-

^a Polymerization conditions: bubbling oxygen in 1,2-dichloroethane at 30 °C for 6 h. Monomer/AMVN = 50/1 by weight. ^b Gel was formed during the polymerization.

Chart 2



with a 5,2-adduct structure is faster than that of the radical with a 5,4-structure; for example, the $\log k_\beta$ values are 2.8 and 5.5 for the 5,4- and 5,2-adducts of **1a**, respectively, being estimated by the equation proposed for the reaction of the allyl radicals with oxygen by Pratt et al.²¹ This result indicates that the reverse reaction (i.e., dissociation) of the 5,2-adduct radical is faster than that of the 5,4-adduct radical by $\sim 10^3$. On the other hand, the reaction with **2a** and **3a** provided a larger BDE_{5,2} value due to the lower electron-withdrawing effect of the amide substituents. For example, the $\log k_\beta$ values are 3.2 and 3.9 for the 5,4- and 5,2-adducts of **2a**, respectively. Namely, the value of

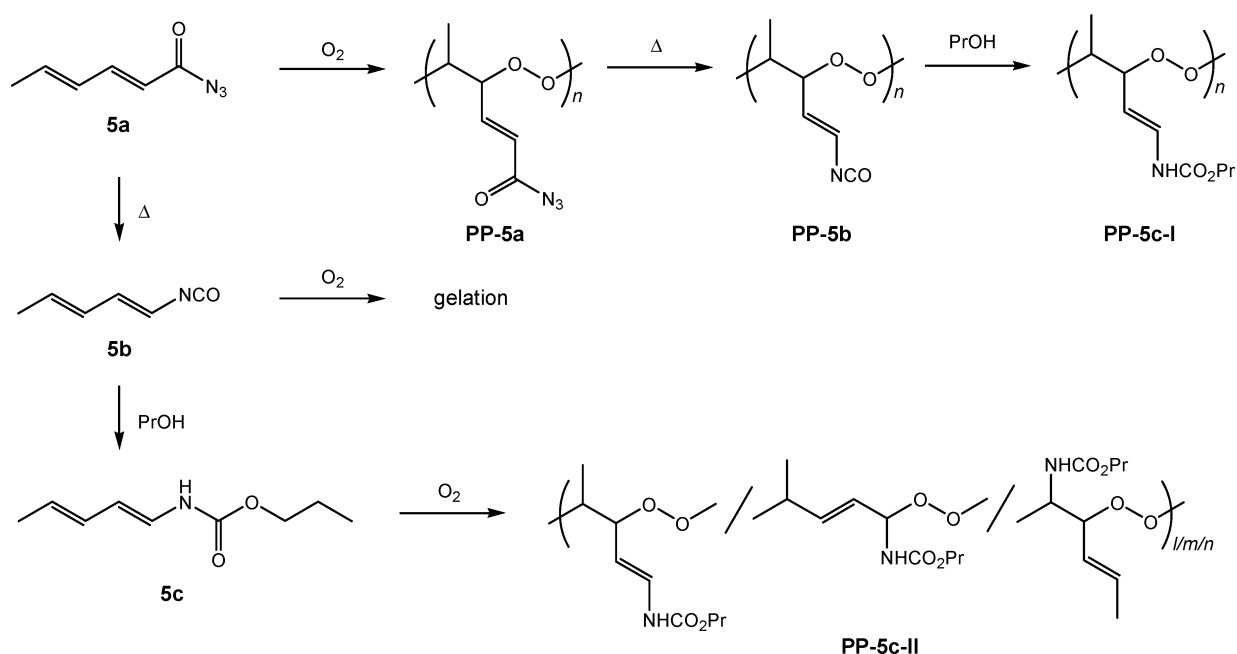
$k_p(5,2)/k_\beta(5,4)$ is 5. These calculation results suggest the possibility that **PP-2** and **PP-3** include not only the 5,4-structure but also the other repeating structures, such as the 5,2- and 2,3-structures, resulting in the irregular polymer repeating structure as well as more complicated degradation reactions. The *N,N*-diphenyl-substituted **3b** exceptionally has a twisted amide conformation, resulting in a propagation selectivity similar to that for the ester derivatives as well as controlled degradation behavior based on the regulated structure of **PP-3b**.

Introduction of Functional Groups into PP. Finally, we tried to demonstrate the synthesis of functional and degradable polymers by introducing any functional group into the side chain of **PP**. There are two methods for the synthesis of the **PP** containing a functional group (Scheme 2). One is the copolymerization of a diene monomer with a functional group, and the other is the polymer reaction of **PP** with a reacting group in the side chain.

Table 4 summarizes the results of the copolymerization of various functional diene monomers with oxygen (Chart 2). All the functionalized monomers **4a–4e** provided the corresponding **PP**, similar to the polymerization of the other ester and amide derivatives **1–3**. However, the monomer concentration was low because of the high molecular weight and the low solubility of these monomers, resulting in the low P_n values. During the copolymerization of **4d** with oxygen, gelation occurred due to the participation of the methacryloyl group in the side chain.

There is another method for the synthesis of the functional **PP** by a polymer reaction, as is shown in Scheme 5. We synthesized **PP** having an azide group **PP-5a**, which can be

Scheme 5



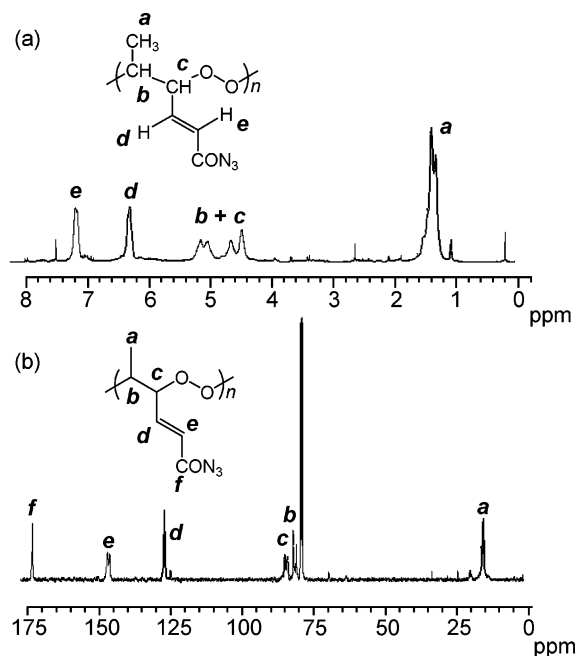


Figure 4. (a) ^1H and (b) ^{13}C NMR spectra of **PP-5a** in CDCl_3 .

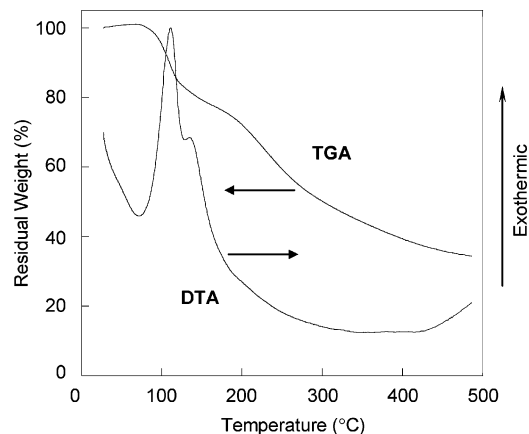


Figure 5. TGA and DTA curves for **PP-5a** in a nitrogen stream at the heating rate of $10\text{ }^\circ\text{C}/\text{min}$.

used for the facile introduction of a variety of functional groups. The azide group rearranges into an isocyanate-containing **PP** (**PP-5b**) accompanied by the evolution of nitrogen by the Curtius rearrangement and then reacts with an alcohol to provide an urethane **PP** (**PP-5c-I**) under mild reaction conditions.^{22–25} **PP-5a** was isolated by precipitation with *n*-hexane in a yield of 25.3%. The M_n and P_n of **PP-5a** were 2.8×10^3 and 16, respectively (Table 4). In the ^1H and ^{13}C NMR spectra of **PP-5a** in Figure 4, the peaks expected as the 5,4-repeating units were exclusively observed, and no peak due to the methylene protons assigned as the 2,3- and 2,5-repeating structures was detected. These results indicate that **5a** copolymerizes with oxygen with a high reactivity and a high selectivity, resulting in the formation of **PP-5a** with a high molecular weight and a well-controlled repeating structure. This is due to the highly conjugating structure of **5a**. We also tried the copolymerization of an isocyanate monomer **5b** with oxygen, but a reactive isocyanate group in the side chain induced gelation during polymerization.

In the TGA/DTA analysis of **PP-5a** (Figure 5), a decrease in weight due to the elimination of N_2 from the azide group was observed around $100\text{ }^\circ\text{C}$; T_{95} and T_{50} are 100.3 and $301.0\text{ }^\circ\text{C}$, respectively. In the DTA curve, two exothermic peaks were

Table 5. Reaction of **PP-5a** with Functional Alcohols

alcohol	[alcohol]/[azide] (mol/mol)	temp ($^\circ\text{C}$)	time (h)	conv (%)
1-propanol	5	30	24	20.1
	10	30	24	28.2
	5	30	36	30.6
	5	30	48	35.5
	5	30	60	34.8
	5	50	3	23.3 ^a
	5	50	5	46.1 ^a
1,2,3,4-tetraacetyl-6-hydroxyglucose (6a)	10	30	24	26.9
2-(9-fluorenyl)ethanol (6b)	10	30	24	27.1
2-hydroxy-2-phenylacetic acid (6c)	10	30	24	25.4 ^b
2-hydroxyethyl methacrylate (6d)	10	30	24	29.9 ^b

^a Partly decomposed. ^b In THF.

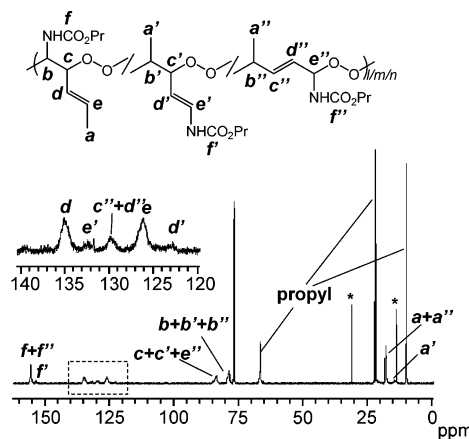


Figure 6. ^{13}C NMR spectrum of **PP-5c-II** obtained by copolymerization of **5c** with oxygen. Measurement solvent, CDCl_3 . An asterisk indicates peaks due to solvents.

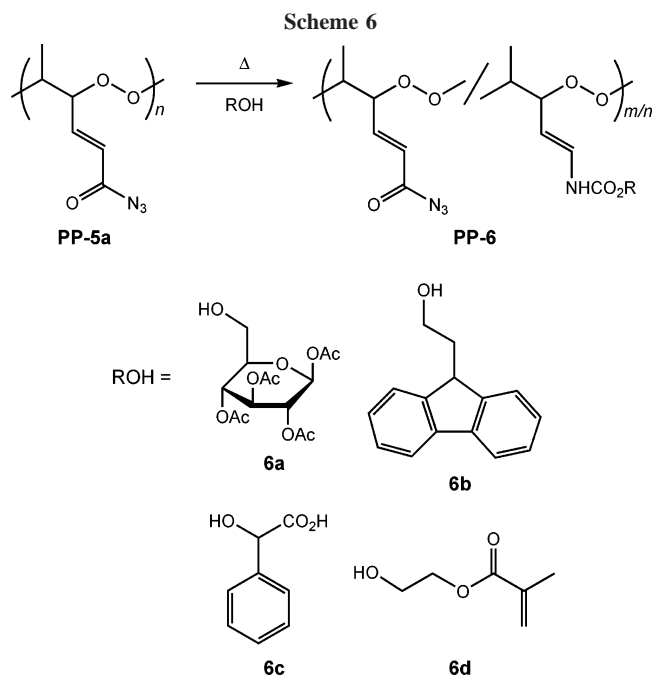
detected due to the thermal degradation of the azide group that rearranged into an isocyanate at $111\text{ }^\circ\text{C}$ and the cleavage of peroxy bonds at $135\text{ }^\circ\text{C}$; $T_{\text{init}} = 71.9\text{ }^\circ\text{C}$ and $T_{\text{max}} = 111.1$ and $134.8\text{ }^\circ\text{C}$. The quite high ΔH (-872 kJ/unit) was observed during the degradation of **PP-5a**.

When the thermal rearrangement of **PP-5a** is carried out in the presence of an alcohol with a functional group, we can expect to obtain a functional **PP**. First, we used 1-propanol as a model compound to examine the reactivity of **PP-5a** toward an alcohol under mild conditions, i.e., at room temperature without any basic or acidic catalyst. **PP-5a** was reacted with an excess amount of 1-propanol in chloroform at $30\text{ }^\circ\text{C}$. In the ^1H NMR spectrum, a peak due to the methine proton was shifted from 7.0 to 6.8 ppm, and additional peaks due to a propyl group were observed after the reaction. As the reaction time was longer and the temperature was higher, the conversion to the urethane increased, but it reached a constant value (35%) after a 48 h reaction (Table 5). The M_n of **PP-5a** slightly increased from 2.8×10^3 to 3.1×10^3 during the reaction with 1-propanol at $30\text{ }^\circ\text{C}$, but the degradation of **PP** partly occurred over $50\text{ }^\circ\text{C}$.

We also examined the structure of **PP-5c-II**, which was obtained from a urethane monomer **5c** by copolymerization with oxygen. The copolymerization results are shown in Table 4. **PP-5c-II** with a high M_n was obtained in a high yield. However, the repeating structure was irregular, as was expected from the structure of **5c**. In the ^{13}C NMR spectrum of **PP-5c-II** (Figure 6), many peaks due to the methine carbons were observed at

123–136 ppm. This supports the formation of the 5,4-, 2,3-, and 2,5-structures as the repeating unit during the copolymerization of **5c**, in contrast to the regular structure of **PP-5a**.

We introduced various functional groups into **PP-5a** in a similar way using several functional alcohols in Scheme 6. A



large excessive amount of the alcohols was reacted with **PP-5a** in chloroform or THF at 30 °C for 24 h. Consequently, functional groups were introduced into the side chain of **PP** at an ~30% conversion, regardless of the kind of alcohols (Table 5). For example, the ^1H NMR spectrum of **PP-6d** is shown in Figure 7. The introduction of a methacryloyl group in the side chain at the conversion of 29.9% was confirmed by the NMR spectrum. The M_n of **PP-6d** was 3.0×10^3 , being slightly higher than that of the precursor **PP-5a** (2.8×10^3). No gelation was observed during the reaction, being different from the synthesis of **PP-4d**.

The methacryloyl group introduced into the side chain of **PP-6d** is further used for the polymerization producing a cross-linking polymer. In fact, the radical copolymerization of **PP-6d** and 2-hydroxyethyl methacrylate in the presence of AMVN as the radical initiator gave a gel, which swells with methanol and dimethylformamide. When the gel was refluxed in toluene

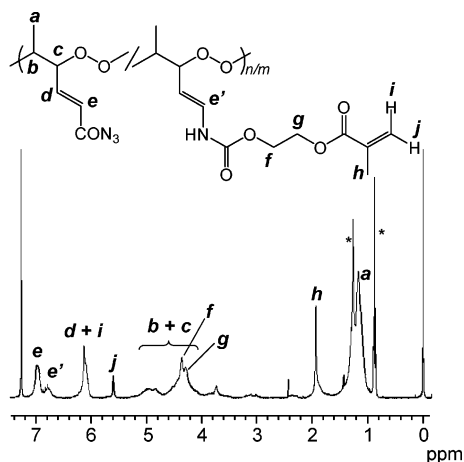


Figure 7. ^1H NMR spectrum of **PP-6d**. Measurement solvent, CDCl_3 . An asterisk indicates peaks due to solvents.

for 1 h, the degradation of a peroxy linkage in the main chain of **PP-6d** proceeded, and the soluble poly(2-hydroxyethyl methacrylate) was recovered by reprecipitation.

Conclusions

We have fabricated **PP** as new types of degradable polymers using 1,3-diene derivatives and oxygen as the starting materials. The exclusive 5,4-propagation is important for determining the thermal degradation property of the alternating copolymers because the existence of the 5,2-structure and other repeating structure is not favored for an efficient degradation. We have confirmed the highly controlled repeating structure of **PP** obtained from ester derivatives, resulting in the well-controlled degradation of **PP**. On the other hand, some amide derivatives provide **PP** containing other repeating units, leading to a more complicated degradation reaction and products. The theoretical approach using the DFT calculation successfully accounted for the selectivity during propagation. The regiospecific addition of a peroxy radical to diene monomers and the regiospecific reaction of an allyl radical with oxygen observed during the copolymerization are attributed to the enthalpies of formation of the allyl radicals and the carbon–oxygen bond dissociation enthalpies of the peroxy radicals, respectively. An amide substituent with a lower electron-withdrawing property was found to disturb the controlled propagation reactions due to the lower selectivity in the reaction of a peroxy radical to a diene and an allyl radical to oxygen. The degradation of **PP** with a controlled repeating unit structure is triggered by various stimuli, which leads to the formation of well-defined products, being of significant potential for a wide range of use in various fields of polymer chemistry and material science including adhesion, coating, environment, and medicinal chemistry. In the present study, we have also demonstrated the synthesis of **PP** including a functional group in the side chain via the direct copolymerization of a functional monomer and the polymer reaction of **PP** including a reactive azide group in the side chain.

Supporting Information Available: Monomer synthesis and spectral data. The material is available free of charge via the Internet at <http://pubs.acs.org>.

References and Notes

- (1) (a) Staudinger, H. *Z. Angew. Chem.* **1922**, 35, 657. (b) Staudinger, H. *Chem. Ber.* **1925**, 58B, 1075.
- (2) Reviews: (a) Bovey, F. A.; Kolthoff, I. M. *Chem. Rev.* **1948**, 42, 491. (b) Mukundan, T.; Kishore, K. *Prog. Polym. Sci.* **1990**, 15, 475. (c) Matsumoto, A. *J. Adhes. Soc. Jpn.* **2003**, 39, 308. (d) Subramanian, K. *J. Macromol. Sci., Polym. Rev.* **2003**, C43, 323.
- (3) (a) Kern, W.; Jockusch, H.; Wolfran, A. *Makromol. Chem.* **1945**, 3, 223. (b) Kern, W.; Heinz, A. R. *Makromol. Chem.* **1955**, 16, 81.
- (4) (a) Miller, A. A.; Mayo, F. R. *J. Am. Chem. Soc.* **1956**, 78, 1017, and the subsequent papers. (b) Mayo, F. R. *J. Am. Chem. Soc.* **1958**, 80, 2465, and the subsequent papers.
- (5) Handy, C. T.; Rothrock, H. S. *J. Am. Chem. Soc.* **1958**, 80, 5306.
- (6) (a) Hendry, D. G.; Mayo, F. R.; Schuetzle, D. *Ind. Eng. Chem. Prod. Res. Dev.* **1968**, 7, 136. (b) Hendry, D. G.; Mayo, F. R.; Jones, D. A.; Schuetzle, D. *Ind. Eng. Chem. Prod. Res. Dev.* **1968**, 7, 145.
- (7) Singh, R. R.; Shrojal, M.; Desai, M.; Sivaram, S.; Kishore, K. *Macromol. Chem. Phys.* **2002**, 203, 2163.
- (8) Nanda, A. K.; Kishore, K. *Macromolecules* **2002**, 35, 6505.
- (9) De, P.; Sathyanarayana, D. N. *Macromol. Chem. Phys.* **2002**, 203, 420.
- (10) Nakano, T.; Nakagawa, O.; Yabe, T.; Okamoto, Y. *Macromolecules* **2003**, 36, 1433.
- (11) (a) Nomura, S.; Itoh, T.; Ohtake, M.; Uno, T.; Kubo, M.; Sada, K.; Miyata, M. *Angew. Chem., Int. Ed.* **2003**, 42, 5468. (b) Itoh, T.; Nomura, S.; Ohtake, M.; Yosida, T.; Uno, T.; Kubo, M.; Kajiwara, A.; Sada, K.; Miyata, M. *Macromolecules* **2004**, 37, 8230.
- (12) (a) Matsumoto, A.; Ishizu, Y.; Yokoi, K. *Macromol. Chem. Phys.* **1998**, 199, 2511. (b) Matsumoto, A.; Higashi, H. *Macromolecules* **2000**, 33,

1651. (c) Hatakenaka, H.; Takahashi, Y.; Matsumoto, A. *Polym. J.* **2003**, 35, 640.
- (13) Matsumoto, A.; Taketani, S. *Chem. Lett.* **2004**, 33, 732.
- (14) Matsumoto, A.; Taketani, S. *J. Am. Chem. Soc.* **2006**, 128, 4566.
- (15) Taketani, S.; Matsumoto, A. *Chem. Lett.* **2006**, 35, 104.
- (16) Taketani, S.; Matsumoto, A. *Macromol. Chem. Phys.* **2004**, 205, 2451.
- (17) Kitamura, T.; Sugimoto, Y.; Matsumoto, A. *12th International Conference on Polymers and Organic Chemistry (POC'06)*, Okazaki, July 2–7, 2006. Kitamura, T.; Matsumoto, A. *Macromolecules*, submitted for publication.
- (18) Matsumoto, A.; Oki, Y.; Otsu, T. *Polym. J.* **1991**, 23, 201, and references therein.
- (19) Odian, G. *Principles of Polymerization*, 4th ed.; Wiley-Interscience: New York, 2004.
- (20) Fujio, R.; Sato, H.; Tsuruta, T. *Kogyo Kagaku Zasshi* **1966**, 69, 2315.
- (21) Pratt, D. A.; Mills, J. H.; Porter, N. A. *J. Am. Chem. Soc.* **2003**, 125, 5801.
- (22) Brochu, S.; Ampleman, G. *Macromolecules* **1996**, 29, 5539.
- (23) Rund, C. J.; Jia, J.; Baker, G. L. *Macromolecules* **2000**, 33, 8184.
- (24) Hua, D.; Cheng, K.; Bai, W.; Bai, R.; Lu, W.; Pan, C. *Macromolecules* **2005**, 38, 3051.
- (25) Scriven, E. F. V.; Turnbull, K. *Chem. Rev.* **1988**, 88, 297.

MA061823X